Supplementary Discussion

Supplementary discussion of steady state kinetic constants. We note that a five amino acid peptide of the consensus sequence identified from a peptide scanning library approach[1] failed to get phosphorylated detectably under our reaction conditions, even when extended to 20 amino acids with a poly-alanine sequence (not shown). That and a subsequent study[2] of short substrate peptides reported substantially lower K_M and higher k_{cat} values than the ones measured here. It is possible these differences are due to the phosphorylation reactions in those studies carried out in the presence of 5 mM Mn^{2+}, whereas our reactions use only Mg^{2+}. Compared to magnesium, manganese is known to substantially lower the K_M values of both the peptide and ATP substrates in canonical kinases[3]. As the intracellular Mn^{2+} concentrations are 2 to 3 orders of magnitude lower than Mg^{2+} (1 to 10 μM for Mn^{2+} and ~1 mM for Mg^{2+})[4], 5 mM Mn^{2+} is unlikely to be a physiologically relevant assay condition for the kinase activity of mTOR.

Supplementary discussion of other mTORC1 substrates in Figure 1g. The substrates we find utilize the FRB-recruitment site are well-established: mTORC1 phosphorylation of GRB10 relieves inhibition of PI3K signaling[1,5], of the LIPIN1 phosphatase stimulates lipogenesis[6], of the TFEB transcription factor inhibits lysosome biogenesis[7], and of MAF1 relieves inhibition of Pol III-mediated transcription[8]. By contrast to these substrates, it is not clear if ULK1, another well-established mTORC1 substrate, utilizes the FRB site. The major ULK1 phosphorylation site (Ser758) is followed by a sequence rich in proline, serine, threonine and glycine residues. In our 20-residue long peptide substrate format, the Ser758-containing peptide gets phosphorylated robustly and at multiple sites, and we could identify mutations that reduce its phosphorylation (not shown).

Supplementary discussion of Raptor structure. The Raptor N-terminus starts with an α helix that packs with the WD40 domain, then the chain traverses the concave surface of the solenoid and transitions into the caspase homology domain. The armadillo repeat domain is very similar to karyopherin alpha, and it can be superimposed on its entirety with a C_α rmsd of 3.9 for 276 residues. The concave surface, where the karyopherin binds to the NLS sequence, binds to two helices (957-978) from the linker between the solenoid and WD40 domains. The Raptor caspase homology domain lacks a functional caspase Cys-His catalytic dyad. The caspase cysteine is replaced by Ser197 (human RAPTOR numbering), and while there is a cysteine immediately before it (Cys196), its side chain is on the opposite side of the β-sheet and points into the hydrophobic core. And, while Raptor has a nearby histidine (His153), it occurs in a loop insertion and is displaced by ~5 Å from the corresponding histidine of caspases. In addition, a loop insertion fills up the caspase fold's substrate-binding site, which previous cryo-EM studies proposed binds to the TOS motif[9,10]. The atRaptor and human RAPTOR structures are very similar except for small rotations (~4° to 7°) between the caspase, solenoid and WD40 domains, which can be individually superimposed with rmsd values in C_α positions of 1.08, 1.02 and 1.4 Å, respectively for 960 out of a total of 1058 residues. The previously published human RAPTOR structure from the 4.4 Å cryo-EM reconstruction of mTORC1 (PDB ID 5h64)[9] has a sequence assignment very different from that of our human RAPTOR structure. In the structure-based alignment of the three domains only two helices (residues 96-114 and 198-219) and a beta strand (145-153) have the same sequence assignment out of 797 residues in that structure. The reported 4 Å crystal structure of *Chaetomium Thermophilum* Raptor (PDB ID 5ef5)[10] is a polyalanine model with un-assigned sequence.

Supplementary discussion of mTORC1 structure. Our 3.0 Å refined mTORC1 structure contains 2204 of 2549 mTOR residues. Three N-heat helices have not been assigned a sequence, and their boundaries

are indicated tentatively (Extended Data Fig. 6). Most of the residues missing from the model are in 6 disordered segments (290-355, 550-577, 904-932, 1223-1260, 1814-1867, 2436-2492). The first four segments are predicted to not have regular secondary structure, except for one predicted helix (327-334) that could not be located in the maps, while the last two segments are also disordered in the $mTOR^{\Delta N}$-mLST8 crystal structure[11]. Only 5 of the model's 57 sequence-assigned helices outside of the $mTOR^{\Delta N}$ crystal structure match the sequence of the reported 4.4 Å cryo-EM structure[9]. In our assignment of the two copies of N-heat, M-heat and FAT-KD to individual mTOR molecules of dimeric mTORC1 (Fig. 4a), the end of N-heat is ~12 Å away from the start of M-heat, a distance that can readily be traversed by the unstructured residues 904 to 932 in between the two solenoids. Thereafter, as the start of M-heat packs with the start of FAT, this head-to-head packing results in the M-heat solenoid extending away from the FAT domain, resulting in a 62 Å distance from the end of M-heat back to the start of the FAT. This distance is traversed by residues 1223-1260, which are mostly unstructured except for forming a short β strand with RAPTOR (Fig. 4a). In apo-mTORC1, the N-terminal half of N-heat becomes progressively disordered towards its N-terminus, and it was built based on its density in RHEB-mTORC1, where it is well ordered.

Supplementary discussion of apo-mTORC1 conformational flexibility. By contrast to RHEB-induced conformational change that is within the FAT domain, the overall conformational flexibility in apo-mTORC1 is due to a hinge motion in the C-terminal portion of N-heat, across ~2 heat repeats that separate the FAT-interacting N-heat end and the mid portion that forms the tripartite interface (Extended Data Fig. 7f). A second, more smoothly varying hinge is within the M-heat, in the portion between the tripartite interface and its N-terminal end that leads to the FAT (not shown). In addition, the N-heat spiral has progressively weaker density towards its N-terminus indicative of it being mobile, presumably because the N-terminal ~2/3rds portion of the spiral is not anchored onto the rest of the structure. This intra- and inter-molecular flexibility is not apparent in the 3D classification of the RHEB-mTORC1 particles (not shown), likely because the N heat spiral is also anchored at its N-terminal end, opposite from its FAT anchor, to M-heat via RHEB. The mobility of the N-terminal portion of the N-heat spiral also suggests how the RHEB-binding site is formed on RHEB binding. We presume that the initial RHEB binding occurs on N-heat, as this interface is the most extensive of the three, accounting for 40 % of the 3930 $Å^2$ total surface area buried, while the RHEB-M-heat/FAT interface and the RHEB-induced N-heat-M-heat interface each account for ~30 %. Once the likely transient RHEB-N-heat subcomplex forms, it may be captured by M-heat during the motion of the N-heat spiral aided by the interchange of inactive conformational states.

References

1 Hsu, P. P. *et al.* The mTOR-regulated phosphoproteome reveals a mechanism of mTORC1-mediated inhibition of growth factor signaling. *Science* **332**, 1317-1322 (2011).

2 Kang, S. A. *et al.* mTORC1 phosphorylation sites encode their sensitivity to starvation and rapamycin. *Science* **341**, 1236566 (2013).

3 Grace, M. R., Walsh, C. T. & Cole, P. A. Divalent ion effects and insights into the catalytic mechanism of protein tyrosine kinase Csk. *Biochemistry* **36**, 1874-1881 (1997).

4 Foster, A. W., Osman, D. & Robinson, N. J. Metal preferences and metallation. *J Biol Chem* **289**, 28095-28103 (2014).

5 Yu, Y. *et al.* Phosphoproteomic analysis identifies Grb10 as an mTORC1 substrate that negatively regulates insulin signaling. *Science* **332**, 1322-1326 (2011).

6 Peterson, T. R. *et al.* mTOR complex 1 regulates lipin 1 localization to control the SREBP pathway. *Cell* **146**, 408-420 (2011).

7 Settembre, C., Fraldi, A., Medina, D. L. & Ballabio, A. Signals from the lysosome: a control centre for cellular clearance and energy metabolism. *Nat Rev Mol Cell Biol* **14**, 283-296 (2013).
8 Michels, A. A. MAF1: a new target of mTORC1. *Biochemical Society transactions* **39**, 487-491 (2011).
9 Yang, H. *et al.* 4.4 A Resolution Cryo-EM structure of human mTOR Complex 1. *Protein & cell* **7**, 878-887 (2016).
10 Aylett, C. H. *et al.* Architecture of human mTOR complex 1. *Science* **351**, 48-52 (2016).
11 Yang, H. *et al.* mTOR kinase structure, mechanism and regulation. *Nature* **497**, 217-223 (2013).

Supplementary Data

Supplementary Figure 1

Figure 1d

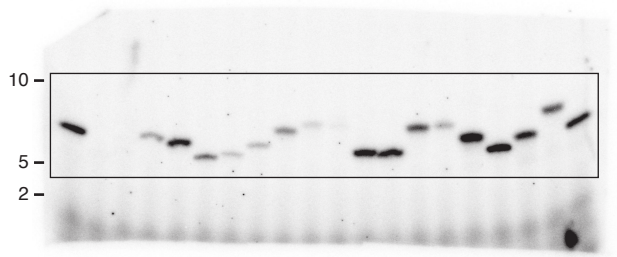

Figure 1e

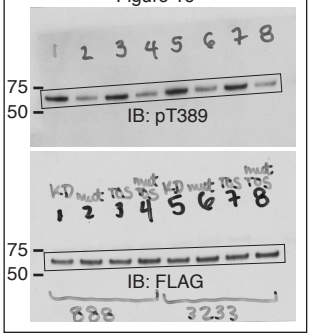

Figure 1f

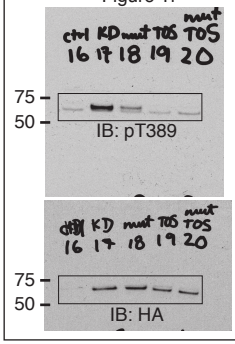

Figure 1g

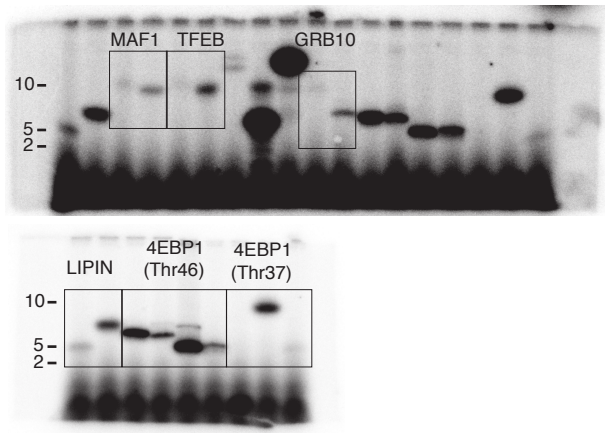

Figure 1h

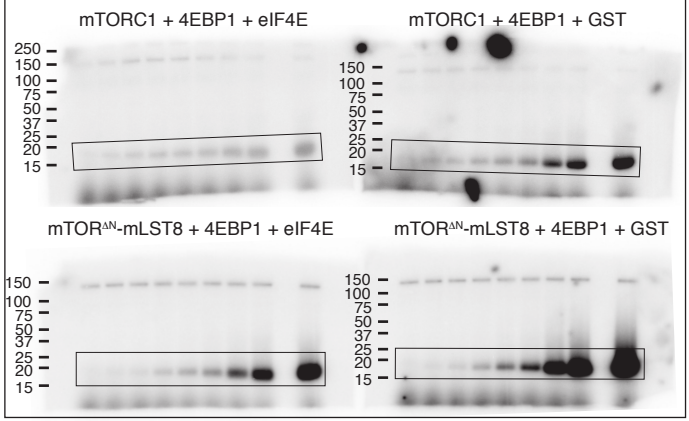

Figure 3a

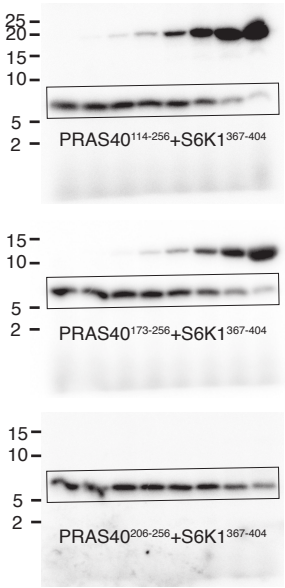

Figure 3e

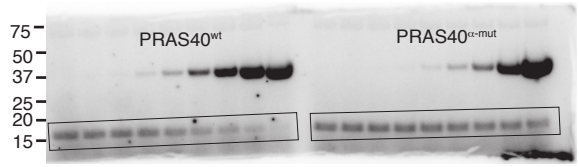

Figure 6b

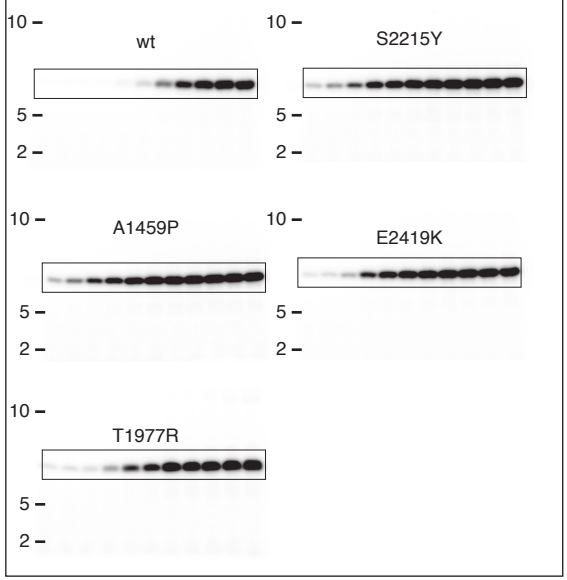

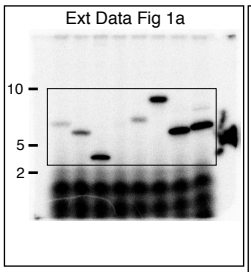
Ext Data Fig 1a
10
5
2

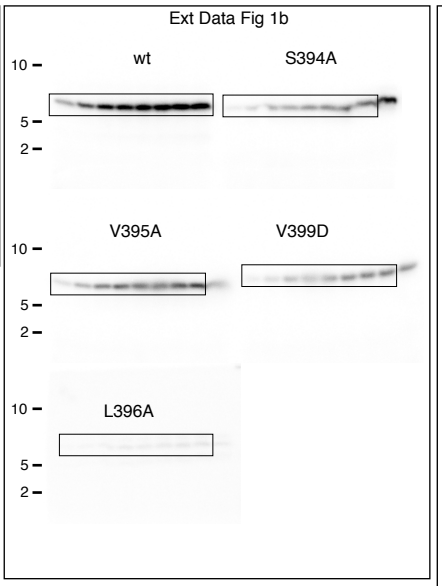
Ext Data Fig 1b
wt
S394A
V395A
V399D
L396A
10
5
2

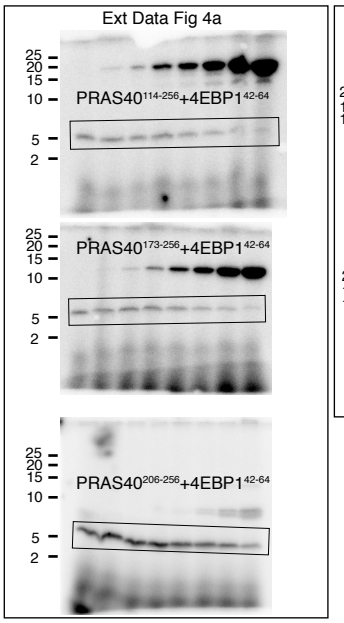
Ext Data Fig 4a
PRAS40114-256+4EBP142-64
PRAS40173-256+4EBP142-64
PRAS40206-256+4EBP142-64
25
20
15
10
5
2

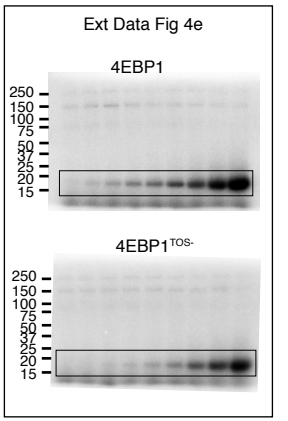
Ext Data Fig 4e
4EBP1
4EBP1TOS-
250
150
100
75
50
37
25
20
15

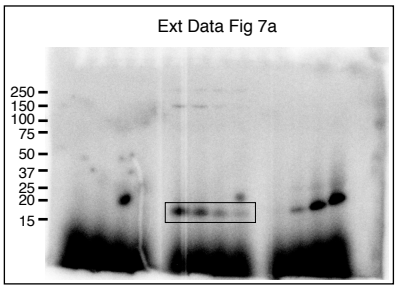
Ext Data Fig 7a
250
150
100
75
50
37
25
20
15

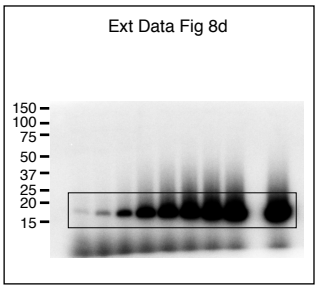
Ext Data Fig 8d
150
100
75
50
37
25
20
15

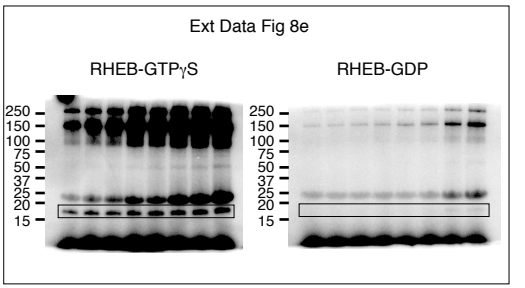
Ext Data Fig 8e
RHEB-GTPγS
RHEB-GDP
250
150
100
75
50
37
25
20
15

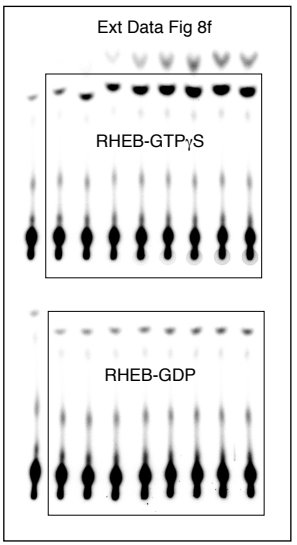
Ext Data Fig 8f
RHEB-GTPγS
RHEB-GDP

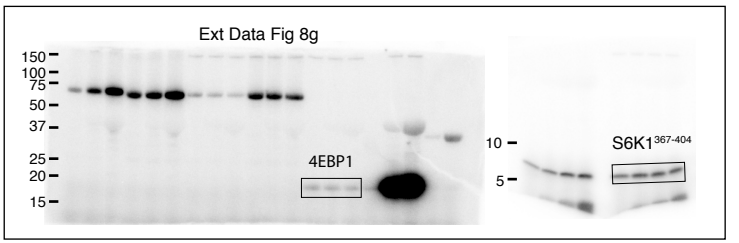
Ext Data Fig 8g
4EBP1
S6K1367-404
150
100
75
50
37
25
20
15
10
5

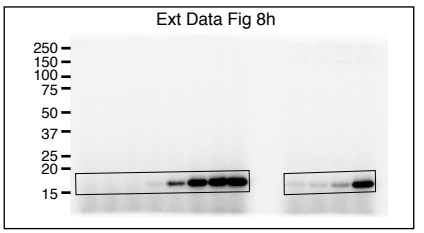
Ext Data Fig 8h
250
150
100
75
50
37
25
20
15

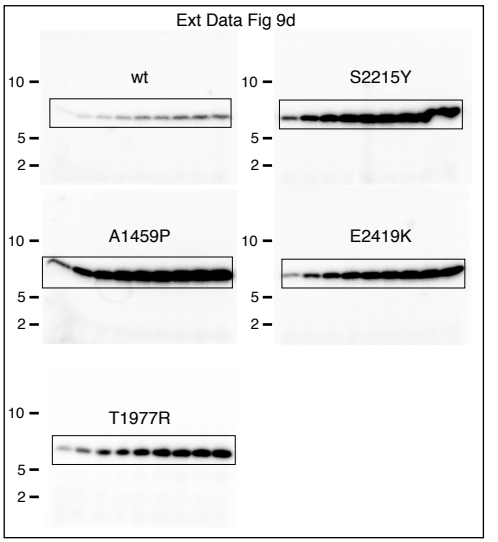
Ext Data Fig 9d
wt
S2215Y
A1459P
E2419K
T1977R
10
5
2

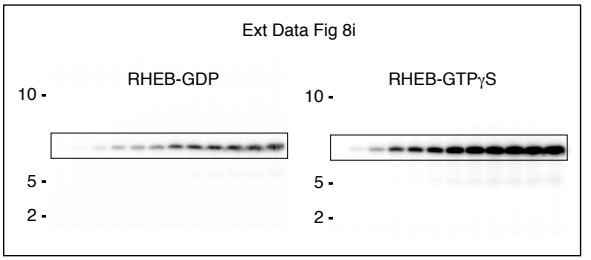
Ext Data Fig 8i
RHEB-GDP
RHEB-GTPγS
10
5
2